Global Change Biology

Global Change Biology (2013) **19**, 798–810, doi: 10.1111/gcb.12079

Spatial patterns and climate drivers of carbon fluxes in terrestrial ecosystems of China

GUI-RUI YU*, XIAN-JIN ZHU*†, YU-LING FU*, HONG-LIN HE*, QIU-FENG WANG*, XUE-FA WEN*, XUAN-RAN LI*†, LEI-MING ZHANG*, LI ZHANG*, WEN SU*, SHENG-GONG LI*, XIAO-MIN SUN*, YI-PING ZHANG‡, JUN-HUI ZHANG§, JUN-HUA YAN¶, HUI-MIN WANG*, GUANG-SHENG ZHOU‖, BING-RUI JIA‖, WEN-HUA XIANG**, YING-NIAN LI††, LIANG ZHAO††, YAN-FEN WANG†, PEI-LI SHI*, SHI-PING CHEN‖, XIAO-PING XIN‡‡, FENG-HUA ZHAO*, YU-YING WANG§§ and CHENG-LI TONG¶¶

**Synthesis Research Center of Chinese Ecosystem Research Network, Key Laboratory of Ecosystem Network Observation and Modeling, Institute of Geographic Sciences and Natural Resources Research, Chinese Academy of Sciences, Beijing, 100101, China, †University of Chinese Academy of Sciences, Beijing 100049, China, ‡Key Lab of Tropical Forest Ecology, Xishuangbanna Tropical Botanical Garden, Chinese Academy of Sciences, Menglun 666303, China, §Institute of Applied Ecology, Chinese Academy of Sciences, Shenyang 110016, China, ¶South China Botanical Garden, Chinese Academy of Sciences, Guangzhou, 510650, China, ‖State Key Laboratory of Vegetation and Environmental Change, Institute of Botany, Chinese Academy of Sciences, Beijing 100093, China, **Faculty of Life Science and Technology, Central South University of Forestry and Technology, Changsha 410004, China, ††Northwest Plateau Institute of Biology, Chinese Academy of Sciences, Xining 810001, China, ‡‡Institute of Agricultural Resources and Regional Planning, Chinese Academy of Agricultural Sciences, Beijing 100081, China, §§Center for Agricultural Resources Research, Institute of Genetics and Developmental Biology, Chinese Academy of Sciences, Shijiazhuang 050021,China, ¶¶Institute of Subtropical Agriculture, Chinese Academy of Sciences, Changsha 410125, China*

Abstract

Understanding the dynamics and underlying mechanism of carbon exchange between terrestrial ecosystems and the atmosphere is one of the key issues in global change research. In this study, we quantified the carbon fluxes in different terrestrial ecosystems in China, and analyzed their spatial variation and environmental drivers based on the long-term observation data of ChinaFLUX sites and the published data from other flux sites in China. The results indicate that gross ecosystem productivity (GEP), ecosystem respiration (ER), and net ecosystem productivity (NEP) of terrestrial ecosystems in China showed a significantly latitudinal pattern, declining linearly with the increase of latitude. However, GEP, ER, and NEP did not present a clear longitudinal pattern. The carbon sink functional areas of terrestrial ecosystems in China were mainly located in the subtropical and temperate forests, coastal wetlands in eastern China, the temperate meadow steppe in the northeast China, and the alpine meadow in eastern edge of Qinghai-Tibetan Plateau. The forest ecosystems had stronger carbon sink than grassland ecosystems. The spatial patterns of GEP and ER in China were mainly determined by mean annual precipitation (MAP) and mean annual temperature (MAT), whereas the spatial variation in NEP was largely explained by MAT. The combined effects of MAT and MAP explained 79%, 62%, and 66% of the spatial variations in GEP, ER, and NEP, respectively. The GEP, ER, and NEP in different ecosystems in China exhibited 'positive coupling correlation' in their spatial patterns. Both ER and NEP were significantly correlated with GEP, with 68% of the per-unit GEP contributed to ER and 29% to NEP. MAT and MAP affected the spatial patterns of ER and NEP mainly by their direct effects on the spatial pattern of GEP.

Keywords: China, driving force, ecosystem respiration, gross ecosystem productivity, net ecosystem productivity, regional carbon budget, spatial variation, terrestrial ecosystems

Received 26 May 2012; revised version received 25 October 2012 and accepted 25 October 2012

Introduction

Since the Industrial Revolution, the intensive human activities have led to continuous increase in atmospheric CO_2 concentration and global warming (Solomon *et al*., 2007). Thus, study on global carbon cycle and carbon budget in terrestrial ecosystems has become one of the key issues in environmental and ecological science (Chapin *et al*., 2006, 2009; Yu *et al*., 2011a). Carbon cycle in terrestrial ecosystems shows large spatial variability due to the impacts from various environmental and biological factors (e.g., climatic variables, vegetation distribution, and land-use change) (e.g., Ciais *et al*., 2000; Beer *et al*., 2010; Deng & Chen, 2011). Therefore, accurately describing the change of carbon

Correspondence: Dr Gui-Rui Yu, tel. +86 10 64889432, fax +86 10 64889432, e-mail: yugr@igsnrr.ac.cn

pools in different regions and quantitatively evaluating the exchange rates among different carbon pools are critical to understand the mechanism of global change and predict the trend of future climate change (Falkowski *et al*., 2000; Houghton, 2007; Yu *et al*., 2011b). Increasing the strength of carbon sink in terrestrial ecosystems is one of the technically and economically feasible ways for the human beings to mitigate climate change (Liu *et al*., 2008). Therefore, the scientific communities are required to quantify the carbon budget and to provide theoretical basis for carbon management in terrestrial ecosystems (Houghton, 2007; Solomon *et al*., 2007; Piao *et al*., 2009).

Currently, several observation and research methods on carbon budget in terrestrial ecosystems are available (Canadell *et al*., 2000; Cao *et al*., 2005; Chapin *et al*., 2006; Chen *et al*., 2008; Yu *et al*., 2011b). Eddy-covariance technique has been widely used to estimate the carbon budget of terrestrial ecosystems at ecosystem, regional, and global scales (Baldocchi *et al*., 2001; Yu *et al*., 2006b; Baldocchi, 2008). For instance, the carbon flux data in different regions have been used to explore the spatial variation and its controlling factors of carbon budget in terrestrial ecosystems in North America (e.g., Law *et al*., 2002; Anderson-Teixeira *et al*., 2011; Bracho *et al*., 2012), Europe (e.g., Valentini *et al*., 2000; Law *et al*., 2002; Lund *et al*., 2010), South America (Keller *et al*., 2004), Asia (Hirata *et al*., 2008; Kato & Tang, 2008), and even globally (Baldocchi, 2008; Yi *et al*., 2010). These data have also been used to simulate the spatial distribution of terrestrial carbon sink and source in North America (Xiao *et al*., 2008, 2010, 2011) and globally (e.g., Beer *et al*., 2010; Yuan *et al*., 2010; Jung *et al*., 2011) by models and other techniques including artificial neural networks and regression trees.

Located in the East Asian monsoon region, China demonstrates a significant temperature gradient from south to north, as well as a significant precipitation gradient from southeast to northwest (Yu *et al*., 2006b). The Qinghai-Tibetan Plateau is an unique geographic unit located in the southwest of China, covering an area of an approximately 2.5×10^6 km^2 with an average altitude of 5000 m above sea level (Royden *et al*., 2008), which has a great impact on the Eurasian atmospheric circulation and climate in China (Ding & Chan, 2005; Wu *et al*., 2007). China is known as an important component of terrestrial ecosystems in the Northern Hemisphere, playing a significant role in maintaining global carbon balance (Fang *et al*., 2007; Piao *et al*., 2009; Pan *et al*., 2011). Therefore, analyzing the regional carbon budget and its spatial patterns in China can help enhance understanding and assessing the carbon budget in regional and global terrestrial ecosystems (Piao *et al*., 2009) and improve our knowledge about ecosystem carbon management.

Since the establishment of Chinese Terrestrial Ecosystem Flux Observation and Research Network (ChinaFLUX) in 2002 (Leuning & Yu, 2006; Yu *et al*., 2006a), the continuous carbon flux measurements have been conducted in major terrestrial ecosystems in China and a large amount of long-term carbon flux data have been acquired. Based on these data, scientists addressed the temporal dynamics and environmental drivers of carbon budget in typical ecosystems (Fu *et al*., 2006; Hao *et al*., 2006; Li *et al*., 2006; Zhang *et al*., 2006; Tan *et al*., 2010, 2011; Wen *et al*., 2010), and analyzed the spatial patterns of carbon fluxes in forest ecosystems (Yu *et al*., 2008) and grassland ecosystems in China (Fu *et al*., 2009) at transect scale. Moreover, soil respiration in China and its spatial pattern were estimated based on network observation on soil respiration rate (Yu *et al*., 2010).

To date, there is still lacking synthetic analysis on the spatial pattern and variation of carbon budget in terrestrial ecosystems in China due to the limit of spatial-temporal representation of observation data in the past few years. Although some previous studies analyzed the spatial patterns of carbon fluxes in Asia (Kato & Tang, 2008) and globally (Baldocchi, 2008; Yi *et al*., 2010), their results were lack of data from China, which greatly constrains the accuracy of Asian and global carbon estimation.

Our objective is to examine the spatial variation and the underlying drivers of carbon budget in terrestrial ecosystems in China by summarizing the long-term flux observation data of ChinaFLUX and published data (GEP, ER, and NEP) from other flux sites in China. We also quantify the statistic characteristics of carbon budget in typical climate zones and major ecosystems in China, and analyze the difference of carbon budget in major ecosystems between China and other regions in the Northern Hemisphere. This study could provide theoretical basis for developing an assessment model of carbon budget in terrestrial ecosystems in Asian and global scales, as well as scientific data support for terrestrial ecosystem carbon sink management.

Materials and methods

Observation technique and data quality evaluation of ChinaFLUX

ChinaFLUX now has grown into a regional observation and research network with 17 sites (Fig. 1), covering four ecosystem types: forest, grassland, cropland, and wetland. Eight of the sites have been conducting continuous flux observation for 10 years. The open-path eddy covariance (OPEC) system

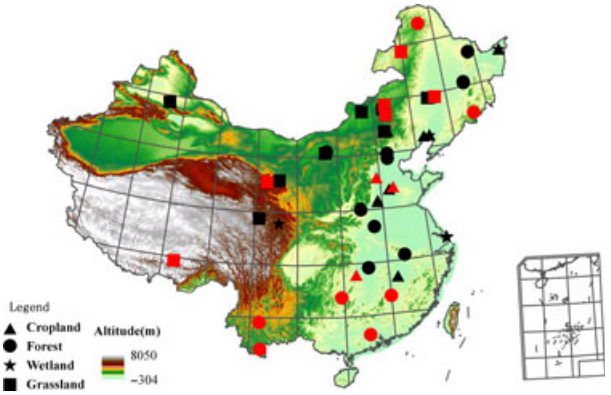

Fig. 1 Distribution of carbon flux observation sites used in this study in China. Note: the data marked in red are sites from ChinaFLUX, background is the 1 km DEM and Qinghai-Tibetan Plateau is in the southwest of China.

was used to measure carbon and water vapor fluxes at ChinaFLUX sites. The OPEC system consisted of a 3D ultrasonic anemometer (Model CSAT-3; Campbell Scientific Inc., Logan, UT, USA) to measure three-dimensional wind speed and temperature fluctuations, and an infrared gas analyzer (Model LI-7500; Licor Inc., Lincoln, NB, USA) to measure CO_2 and water vapor densities. All signals were sampled at a frequency of 10 Hz and the CO_2 and H_2O fluxes were calculated and recorded at 30 min intervals by a CR5000 datalogger (Model CR5000; Campbell Scientific Inc.). The meteorological variables were measured simultaneously at each site, including solar radiation, air temperature, rainfall, soil temperature, and soil moisture, which were sampled at a frequency of 2 s and recorded at 30 min intervals. See Yu *et al.* (2006a) for the detailed information for the instruments at different ecosystems.

Although energy closure is affected by many factors, it is still a key indicator to assess the quality of flux data (Massman & Lee, 2002; Wilson *et al.*, 2002; Wen *et al.*, 2005). Li *et al.* (2005) and Tan *et al.* (2010) examined the energy closure at different sites of ChinaFLUX. Their results showed that energy closure at all ChinaFLUX sites exceeded 0.7, indicating those measurements are reasonable.

Data processing method

To ensure the reliable processing of flux data, ChinaFLUX developed a series of proven methodologies for assessing the performance of observation system and flux data quality control including coordinate rotation, WPL correction, canopy storage calculation, nighttime flux correction, and gap filling and flux partitioning (Yu *et al.*, 2006a).

Prior to conducting the scalar flux computation, three-dimensional rotation of the coordinate was applied to wind components to remove the effect of instrument tilt or irregularity on airflow (Zhu *et al.*, 2005). The WPL correction was then applied to adjust the effect of air density caused by the transfer of heat and water vapor with the method described by Webb *et al.* (1980). Storage flux was calculated and the abnormal values were eliminated. The nighttime CO_2 flux data under low atmospheric turbulence conditions were screened using site-specific thresholds of friction velocity (u_*), which was identified with the method described by Reichstein *et al.* (2005). The data gaps were filled with the nonlinear regression method suggested by Falge *et al.* (2001) and NEE was partitioned into GEP and ER with the method described by Reichstein *et al.* (2005). See Yu *et al.* (2006a) for the details of data quality control and gap filling.

Collection and integration of carbon flux observation data

Besides the long-term observation from ChinaFLUX sites, the carbon flux data of other sites in China were also collected from literature. Only the sites with at least 1 year continuous flux measurements were selected for calculating annual statistics of GEP, ER, NEP, and climatic variables [mainly mean annual temperature (MAT) and mean annual precipitation (MAP)]. If sites in the literature did not have solar radiation data, we used the interpolated long-term solar radiation from Zhu *et al.* (2010).

No flux measurements data were available during wintertime in ecosystems in cold temperate zones. However, such ecosystems usually represent one of the unique eco-regions and play an important role in spatial pattern analysis. Thus, the data of these sites were also included. Considering the small contribution of ER during nongrowing seasons to annual total carbon budget in these ecosystems, the data measured during growing seasons were used to represent annual value.

Totally, 52 sites were included in this study (Table S1), covering 18 forest sites, 15 grassland sites, 7 wetland sites, and 12 cropland sites (Fig. 1), which almost covered the major eco-regions and typical ecosystem types in China. In the sites only having 1 year data, the observed fluxes and climatic variables were directly used in this analysis. In the other sites having longer than 1 year data, we calculated the average of carbon fluxes and climatic variables during the measuring periods. As for sites missing climatic data, we used multiyear average climatic data as the substitution. Besides, some sites from literature included NEP, GEP, or ER incompletely, so that the site number used for analyzing the spatial patterns of GEP, ER, and NEP was unequal.

To analyze the difference of carbon fluxes between China and other regions in the Northern Hemisphere such as the United States, Canada, and Europe, we also collected the published carbon flux data of different terrestrial ecosystems in those regions, which included 152 sites (the United States: 51, Canada: 32, Europe: 69, data were not shown). If sites have more than 1 years' data, the average values for carbon fluxes were calculated. Then, those data were classified to four types of ecosystem (Forest, Grassland, Wetland, and Cropland) and compared with these in China.

Statistic analysis

The above computations were done with MATLAB software (Math Works Inc., Natick, MA, USA). Under Matlab 7.7, the generalized linear model (GLM) of regstats was used to

conduct the regression analyses between carbon fluxes and longitude, latitude and climatic variables and test the significance of the regressions, which were also conducted with nonlinear regression such as the exponential regression. By comparing the R^2 and root mean squared error (RMSE), we selected the better-fit functions that had a higher R^2 and lower RMSE. The stepwise regression was used to analyze the binary linear regression on carbon fluxes with MAT and MAP and the interaction between MAT and MAP. In the stepwise regression, the minimum P-value for a variable to be recommended for adding to and removing from the model was 0.10. The path-analysis was conducted to evaluate the dependence of the spatial variations of carbon fluxes on climatic factors. With one-way analysis of variance (ANOVA), the significance test on the difference of carbon budget between China and other regions was conducted and the significance level was at $\alpha = 0.05$.

Results

Zonal distribution of climatic factors in China

The trends of MAT and MAP along the longitude and latitude for the flux sites in China were shown in Fig. 2. It can be seen that except the sites with an altitude over 2000 m, the MAT declined significantly with the increase of latitude at other sites. MAT decreased by 0.85 °C with 1° increase of latitude, and all data fell in the 95% confidence interval (Fig. 2a). This was also the case for MAP, which decreased by 40.4 mm for 1° increase of latitude (Fig. 2b). MAT and MAP did not exhibit significant longitudinal trends (Fig. 2c,d). Figure 2 also indicates that the Qinghai-Tibetan Plateau had a significant impact on the latitudinal pattern of MAT (Fig. 2a). The MAT at the flux sites on the Qinghai–Tibetan Plateau was significantly lower than that in low-altitude areas at the same latitude (Fig. 2a).

Statistic characteristics of carbon budget of major ecosystems in China

Based on the flux dataset obtained from the 52 sites (Table S1), we estimated the carbon budgets of forest, grassland, and wetland ecosystems in typical climate zones in China (Table 1).

In general, the forest ecosystems in China had a relatively large C sequestration capacity. The NEP of forest ecosystems in China ranged from 168.8 to 592.4 gC m^{-2} yr^{-1}, with the largest carbon sink in central subtropical forest. The NEP in warm temperate forest, northern subtropical forest, and southern subtropical forest ranged from 385 to 510 gC m^{-2} yr^{-1}. The tropical forest exhibited as a weak carbon sink,

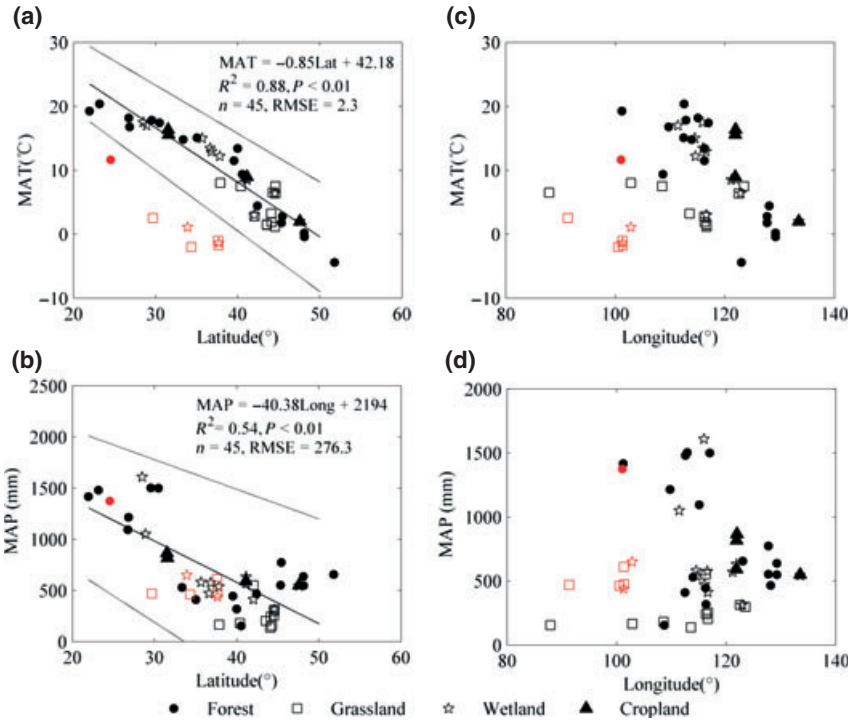

Fig. 2 Trends of MAT and MAP along latitude and longitude for different terrestrial ecosystems in China, where MAT is mean annual temperature, and MAP is mean annual precipitation. The thick line is the regression line, and the thin lines are the 95% confidence interval. Note: the data marked in red are generated from the observation sites with an altitude over 2000 m.

Table 1 Statistic features of carbon fluxes of forest, grassland, and wetland ecosystems in key regions in China

Types of ecosystems	Climate zones	Representative regions	Mean annual GEP ($gC\ m^{-2}\ yr^{-1}$)	Mean annual ER ($gC\ m^{-2}\ yr^{-1}$)	Mean annual NEP ($gC\ m^{-2}\ yr^{-1}$)	Observation number (n)	Observation sites where the data were generated
Forest	Cold temperate forest	Northern Daxing'anling	962.75	760.40	242.35	1	HZ
	Central temperate forest	Central temperate forest*	1007.15 ± 568.54	822.85 ± 507.74	191.75 ± 72.03	6	YCF, YCF2, CBS, LS, KBQF, MES
	Warm temperate forest	Warm temperate forest†	1406.55 ± 167.51	1013.85 ± 69.51	385.36 ± 117.81	4	DXF, XLD, XP, HD
	Northern subtropical forest	Northern subtropical forest‡	1917	1406.13	510.88	2	AQ, YY
	Central subtropical forest	Central subtropical forest§	1639.69 ± 319.39	1047.20 ± 232.57	592.36 ± 343.59	3	QYZ, ALS, HT
	Southern subtropical forest	Southern subtropical forest¶	1367.26	971.31	395.95	1	DHS
	Tropical forest	South of Tropic of Cancer	2342.67	2173.83	168.83	1	XSBN
Grassland	Alpine steppe-meadow	Hinterland of Qinghai-Tibetan Plateau	197.46	207.65	-10.18	1	DX
	Alpine meadow	Eastern edge of Qinghai-Tibetan Plateau	563.14 ± 77.75	492.19 ± 36.54	113.65 ± 93.33	4	SJY, HB, HBGC, HTC
	Temperate desert steppe	West of Inner Mongolia	270.18	221.01	49.17	1	KBQG
	Temperate steppe	Central and eastern parts of Inner Mongolia	225.80 ± 85.93	251.91 ± 85.59	-17.65 ± 82.47	6	XLHT, NM, XLF, XLD, DLG, XLGL
	Temperate meadow steppe	Songnen Plains	396.41	375.8	112.35	2	TYG, CL
Wetland	Mire-wetland	Sanjiang Plains	497	453	61.67	1	SJS
	Alpine wetland	Zoige Plateau, Qinghai-Tibetan Plateau	560.03	567.90	-7.86	2	HBSD, Zoige
	Coastal wetlands	The delta of Liaohe and Yangtze River	1552.61 ± 218.64	1092.34 ± 120.80	460.94 ± 285.98	4	PJ, DTD, DTZ, DTG

The error interval means the standard deviation of carbon fluxes in the same climate zone. Limited to the observation number, some climate zones with lower than three observations does not have the error interval.

*Central temperate forest: Songliao Plains in the north of Shenyang, eastern part of northeastern China, northern Yanshan, and Yinshan Mountains, northern Xinjiang.

†Warm temperate forest: Southern part of northeastern China in the south of Shenyang, North China Plains, Shandong Peninsular, southeast of Loess Plateau, and southern Xinjiang.

‡Northern subtropical forest: The areas between Qinling Mountain Range and Daba Mountain, the plains in the middle and lower reaches of Yangtze River.

§Central subtropical forest: Hilly areas between southern Yangtze River and Nanling Mountain Range, mountainous areas in Zhejiang and Fujian provinces, central and northern Guangxi, northern Guangdong, northern Taiwan, Sichuan Basin, partial areas in Yunnan-Guizhou Plateau, and southeastern Qinghai-Tibetan Plateau.

¶Southern subtropical forest: The areas between south of Nanling Mountain Range and Tropic of Cancer.

with the NEP value of 168.8 gC m^{-2} yr^{-1}. The highest GEP occurred in the tropical forest at XSBN, followed by the northern subtropical forest and the central subtropical forest. The GEP in the southern subtropical forest was comparable with that in the warm temperate forest, whereas that in the central temperate forest and cold temperate forest were relatively low. The spatial pattern of ER was similar to that of GEP, with the highest ER appeared at the tropical forest, and followed by the northern subtropical, the central subtropical and the warm temperate forests.

Grassland ecosystems had generally weaker carbon sequestration capacity than forest ecosystems, with a significant regional difference. The temperate meadow steppe in northeast China showed the largest carbon sink, with a mean annual NEP up to 112.4 gC m^{-2} yr^{-1}. The alpine meadow in the eastern edge of Qinghai-Tibetan Plateau also exhibited strong carbon sink. However, temperate steppes in Inner Mongolia and the alpine steppe-meadow in the hinterland of Qinghai-Tibetan Plateau were characterized as carbon neutral or weak carbon source. The GEP of alpine meadow was the highest (up to 563.1 $\pm$ 77.8 gC m^{-2} yr^{-1}), whereas that of grasslands in other regions was relatively low, with the minimum GEP occurred in the alpine steppe-meadow at DX (only 197.46 gC m^{-2} yr^{-1}). The spatial pattern of ER in grasslands was similar to that of GEP.

The wetland ecosystems are scatteredly distributed across China, including the alpine wetland, coastal mudflat, mire-wetland, constructed wetlands, and so on. The carbon sequestration capacity of wetland ecosystems showed a significant spatial variation. The coastal wetlands, located in the delta of the Liaohe and the Yangtze River, showed the strongest carbon sink, with the NEP exceeding 400 gC m^{-2} yr^{-1}. The NEP of mire-wetland in the Sanjiang Plains was 161.8 gC m^{-2} yr^{-1}. The alpine wetlands showed a large difference in NEP, with HBSD acting as a carbon source (−79.1 gC m^{-2} yr^{-1}) but Zoige as a carbon sink (63.4 gC m^{-2} yr^{-1}). The GEP in coastal wetlands was the largest (up to 1500 gC m^{-2} yr^{-1}), whereas that of wetland in the Sanjiang Plains and the Qinghai-Tibetan Plateau was around 500 gC m^{-2} yr^{-1}. In the wetlands, the spatial variation of ER was similar to that of GEP.

The difference of carbon fluxes (GEP, ER, and NEP) between China and other regions in the North Hemisphere was shown in Fig. 3. The NEP of most ecosystems in China was positive, which was similar to that in the United States, Canada, and Europe (Fig. 3c). NEP of all ecosystem types in China was 252.9 $\pm$ 234.2 gC m^{-2} yr^{-1}, higher than that in the United States and Europe in magnitude (Fig. 3c). However, this difference was not significant at the significant level of 0.05. The carbon fluxes of forest ecosystems in different regions also exhibited significant differences (Fig. 3d–f). NEP of forest ecosystems in China was 349.9 $\pm$ 207.7 gC m^{-2} yr^{-1}, higher than those in Europe, the United States, and Canada. However, this difference among China, Europe, and the United States was not statistically significant ($P > 0.05$) (Fig. 3f). The GEP of forest in China, the United States, and Europe was comparable, but higher than those in Canada (Fig. 3d), while there was no significant difference in ER for the forest ecosystems among regions. The carbon fluxes of grassland ecosystems were significantly lower than those of forest, particularly in the grasslands in China, the United States, and Canada (Fig. 3g–i). The difference of NEP of grassland ecosystems in different regions was not statistically significant, whereas the GEP values of grasslands in Europe and the United States were significantly higher than those in China and Canada (Fig. 3g). However, carbon fluxes of wetland and cropland ecosystems were smaller than those of forest ecosystems, but larger than grassland ecosystems (Fig. 3j–o) and showed no significant differences among regions.

Latitudinal and longitudinal patterns of GEP, ER, and NEP

The zonality of hydrothermal conditions at continental scale has resulted in the regional differentiation of climatic factors, and has a profound impact on the spatial pattern of carbon budget of terrestrial ecosystems in China. GEP, ER, and NEP of terrestrial ecosystems across China exhibited significant latitudinal patterns (Fig. 4a), and that trend was not altered when different vegetation types were included. In general, GEP, ER, and NEP declined linearly with the increase of latitude ($P < 0.01$) (Fig. 4a). With the regression model, the RMSE for GEP, ER, and NEP was 515.2, 404.2, and 201.3 gC m^{-2} yr^{-1}. With 1° increase of latitude, GEP decreased by 54.2 gC m^{-2} yr^{-1}, while ER and NEP decreased by 33.2 and 16.9 gC m^{-2} yr^{-1}. The NEP dropped below zero when latitude exceeds 53.2°, indicating a carbon source in high latitudes.

The complex longitudinal distribution of climatic factors in different regions of China resulted in the complex distribution of GEP, ER, and NEP, leading to the no clear longitudinal trend in carbon fluxes (Fig. 4b). The spatial distribution of carbon fluxes in the southwest and northwest in the same longitude differed greatly due to the impact of the Qinghai-Tibetan Plateau, which results in a dry climate in northwest China and a moist climate over south China (Wu *et al.*, 2007), thus weakening the longitudinal distribution

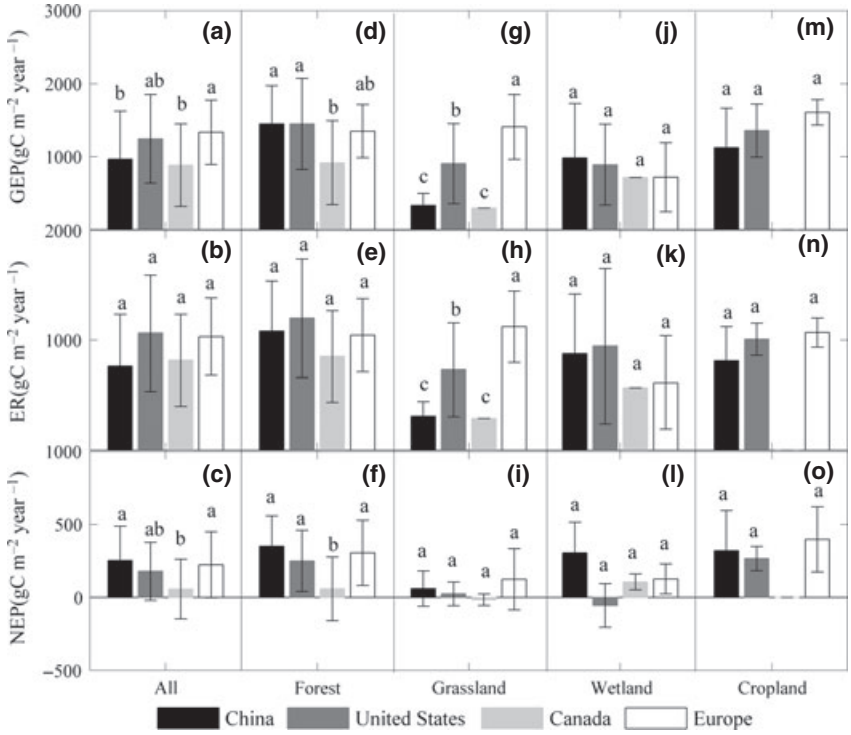

Fig. 3 Statistical characteristics of carbon fluxes in different countries and regions. GEP, ER, and NEP are the abbreviation of gross ecosystem productivity, ecosystem respiration, and net ecosystem productivity, respectively.

patterns of carbon fluxes in different regions of China (Fig. 4b). When ecosystems in Qinghai-Tibetan Plateau, in Inner Mongolia and northwest regions (mostly arid area) (the observation data circled with dotted lines in Fig. 4b) were excluded to eliminate the impact of the Qinghai-Tibetan Plateau, the carbon fluxes in other ecosystems declined significantly in a linear way with the increase of longitude ($P < 0.01$).

Correlation of spatial patterns in GEP, ER, and NEP

There are many studies well demonstrating the correlation among GEP, ER, and NEP of typical ecosystems and its mechanism (Lasslop *et al.*, 2010). A key finding in this study was that the spatial patterns of GEP, ER, and NEP of all terrestrial ecosystems in China (consisting of forest, grassland, wetland, and cropland ecosystems) also showed an obvious 'positively coupling correlation' (Fig. 5), i.e., a strong linear relationship existed between GEP and NEP or ER. Their regression coefficients were both significant ($P < 0.01$) and nearly all sites fell into the 95% confidence interval. The RMSE for regressed ER and NEP was 153.4 and 169.3 gC m^{-2} yr^{-1}, respectively. Therefore, ER and NEP of the regional terrestrial ecosystems in China were dominantly determined by annual GEP. In terms of spatial pattern variation, the per-unit of GEP contributed 68% to ER, and 29% to NEP.

Impact of climate factors on the spatial patterns of GEP, ER, and NEP

There were many climate factors affecting the spatial patterns of carbon fluxes. We analyzed the relationship between climate variables (MAT, MAP, mean annual radiation (MAR)) and carbon fluxes (GEP, ER, and NEP). Results from the path-analysis (Fig. 6) showed that the direct effects of MAT and MAP were similar in shaping the spatial patterns of GEP and ER, which were higher than that of MAR in magnitude. While the spatial pattern of NEP was largely affected by the direct effect of MAT, which was higher than that of MAP and MAR. Thus, we used MAT and MAP as the main driving factors to analyze the spatial patterns of carbon fluxes.

Firstly, we analyzed the effect of single factor (MAT or MAP) on the spatial patterns of GEP, ER, and NEP. GEP and NEP grew linearly while ER grew exponentially with the increase of MAT. While few relative low air temperature sites fell out of the 95% confidence interval (Fig. 7a–c). The R^2 was 0.57, 0.49, and 0.48 for GEP, ER, and NEP, respectively. Meanwhile, the RMSE for the regressed GEP, ER, and NEP was only 435.1,

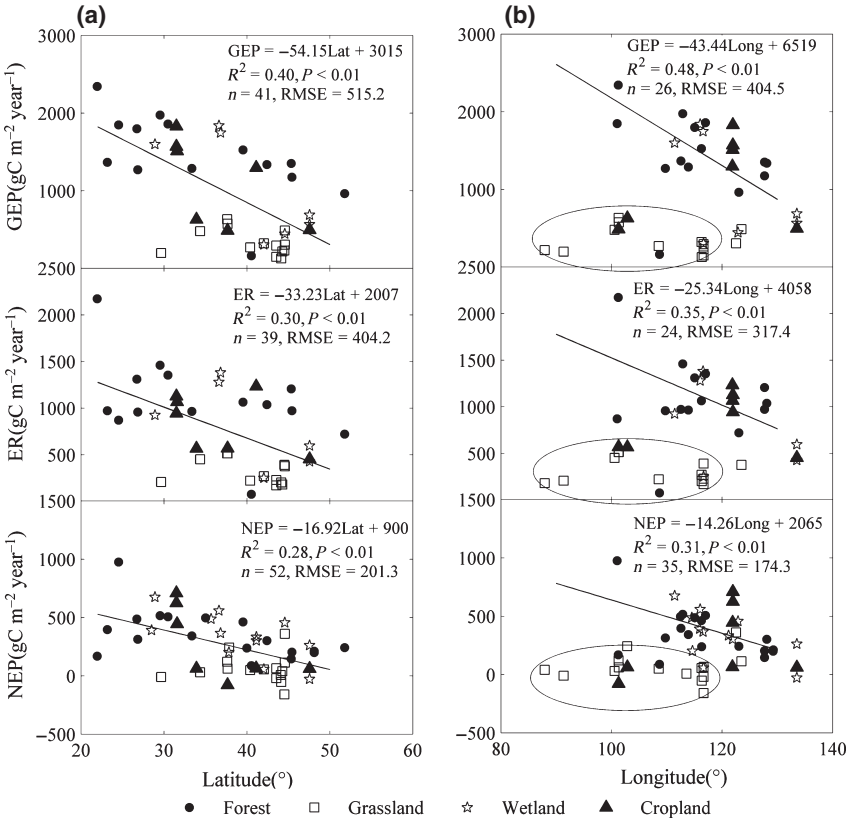

Fig. 4 The relationships between GEP, ER, and NEP in terrestrial ecosystems in China with (a) latitude and (b) longitude, where GEP, ER, and NEP are gross ecosystem productivity, ecosystem respiration and net ecosystem productivity, respectively. The 95% confidence interval is not shown in this figure as all sites fell in the intervals. Note: Observation sites circled by the thin lines in the longitudinal trend include the sites in Inner Mongolia, Qinghai-Tibetan Plateau and northwest regions, while the fitted straight lines indicate the relationship of site-based observation data and the longitudes in east China.

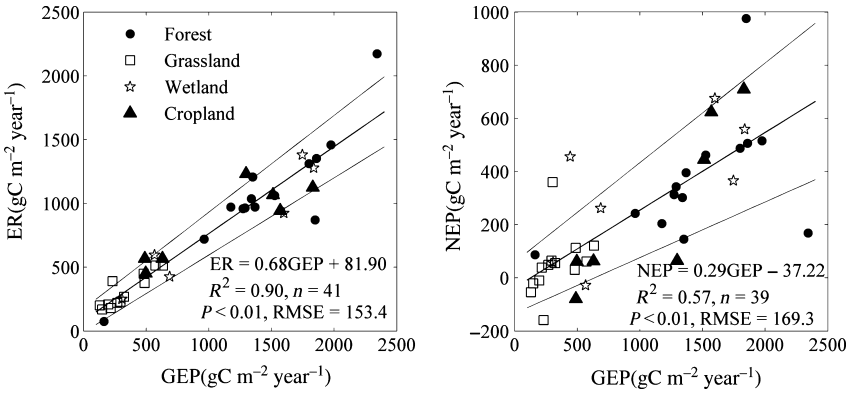

Fig. 5 Coupled relations between GEP, and ER and NEP in spatial patterns. GEP, ER, and NEP are gross ecosystem productivity, ecosystem respiration, net ecosystem productivity, respectively. The thick line is the regression line, and the thin lines are the 95% confidence interval.

342.1, and 170.2 gC m^{-2} yr^{-1}, respectively. For every degree increase in MAT, GEP increased by 69.1 gC m^{-2} yr^{-1} and NEP increased by 23.4 gC m^{-2} yr^{-1}, indicating that the region with higher MAT had stronger carbon sequestration capacity. As the increase in MAP, GEP, ER, and NEP grew significantly in a linear way. However, some sites with MAP between 400 and 700 mm fell out of the 95% confidence interval (Fig. 7d–f).

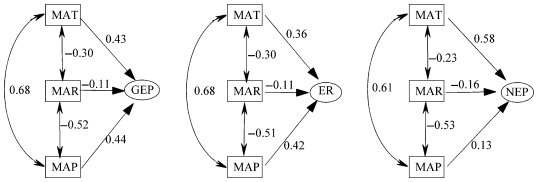

Fig. 6 Path diagram illustrating the changing effects on climate variables related to the spatial patterns of carbon fluxes in China. Standardized correlation coefficients are labeled in the Figure. GEP, ER, and NEP are gross ecosystem productivity, ecosystem respiration, and net ecosystem productivity, respectively. MAT, MAP, and MAR are the mean annual temperature, mean annual precipitation and mean annual radiation, respectively.

MAP contributed 61%, 51%, and 32% to the spatial variations in GEP, ER, and NEP, respectively. The RMSE for the regressed GEP, ER and NEP was only 413.7, 335.9, and 194.7 gC m^{-2} yr^{-1}, respectively. For every 100 mm growth in MAP, GEP increased by 129.7 gC m^{-2} yr^{-1}, whereas ER and NEP increased by 84.9 and 34.0 gC m^{-2} yr^{-1}, respectively.

Secondly, we conducted a binary linear regression analysis on carbon fluxes with MAT and MAP, and found that the combined contribution of MAT and MAP to the spatial variations in GEP, ER, and NEP increased significantly compared with the single-factor contribution of MAT or MAP. MAT and MAP jointly explained 71% of the spatial variation of GEP, which was 10% higher than that of single factor (MAT or MAP), and the RMSE reduced from 413.7 to 364.3 gC m^{-2} yr^{-1}. The combined contribution of MAT and MAP to the spatial variations of ER and NEP also increased to 58% and 52%, the RMSE reduced from 335.9 to 317.1 gC m^{-2} yr^{-1} for ER and from 170.2 to 166.3 gC m^{-2} yr^{-1} for NEP.

Furthermore, we carried out a quadratic regression analysis by taking into account the impact of the interaction between MAT and MAP on carbon fluxes. The results showed that the interaction between MAT and MAP had a significant impact on the regional carbon fluxes in China. Particularly, the regression equation significantly improved the explanation on the spatial

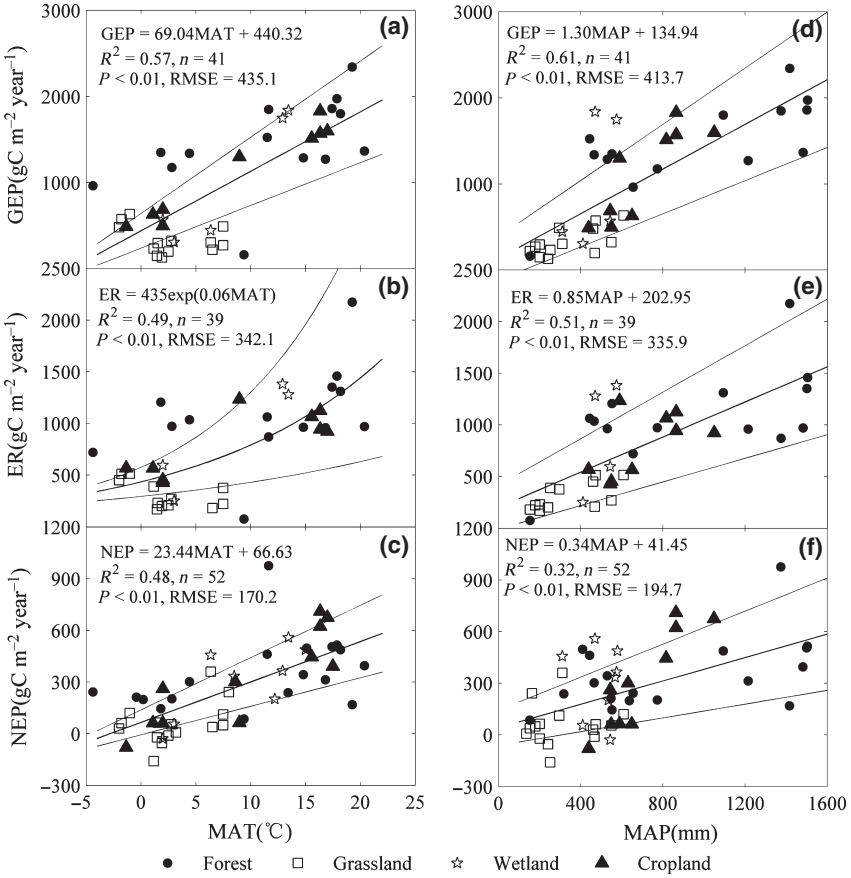

Fig. 7 The relationships between climate variables (MAT and MAP) and GEP, ER, and NEP in different ecosystems in China. GEP, ER, and NEP are the abbreviation of gross ecosystem productivity, ecosystem respiration and net ecosystem productivity, respectively. MAT and MAP are the mean annual temperature and mean annual precipitation. The thick line is the regression line, and the thin lines are the 95% confidence interval.

variations of GEP and NEP and decreased the RMSE. By integrating the interaction between MAT and MAP, the explanation of the regression equation to GEP increased from 71% to 79%, and the RMSE decreased from 364.3 to 313.9 gC m^{-2} yr^{-1}. Integrating the interaction between MAT and MAP also increased the explanation of NEP from 52% to 66% and decreased the RMSE from 166.3 to 141.6 gC m^{-2} yr^{-1}. The impact of such interaction between MAT and MAP on GEP and NEP was statistically significant ($t = -4.42$, $P < 0.01$; $t = -3.76$, $P < 0.01$). After taking the interaction of MAT and MAP on ER into account, R^2 increased from 0.58 to 0.61 and RMSE reduced from 317.1 to 308.1 gC m^{-2} yr^{-1}. Therefore, based on these analyses, we recommend using the following three regression equations to describe the spatial patterns of GEP, ER, and NEP in terrestrial ecosystems in China.

$$\begin{aligned} \mathrm{GEP} = {} & 107.02\mathrm{MAT} + 2.18\mathrm{MAP} - 0.10\mathrm{MAT} \times \\ & \mathrm{MAP} - 544.35, \\ & R^2 = 0.79, n = 41, \mathrm{RMSE} = 313.9 \end{aligned} \quad (1)$$

$$\begin{aligned} \mathrm{ER} = {} & 54.08\mathrm{MAT} + 1.19\mathrm{MAP} - 0.05\mathrm{MAT} \times \\ & \mathrm{MAP} - 103.04, \\ & R^2 = 0.61, n = 39, \mathrm{RMSE} = 308.1 \end{aligned} \quad (2)$$

$$\begin{aligned} \mathrm{NEP} = {} & 48.98\mathrm{MAT} + 0.79\mathrm{MAP} - 0.05\mathrm{MAT} \times \\ & \mathrm{MAP} - 313.85, \\ & R^2 = 0.66, n = 52, \mathrm{RMSE} = 141.6 \end{aligned} \quad (3)$$

Discussion

Statistical characteristics of carbon fluxes of different ecosystems in China

This study analyzed the statistical characteristics of carbon fluxes in different ecosystems in China, which were compared with those in other regions in the Northern Hemisphere. These data provided valuable information to assess the carbon budget of terrestrial ecosystems worldwide, particularly in Asia.

The positive NEP of most ecosystems in China, the United States, Canada, and Europe, meaning that the major terrestrial ecosystems in these regions are acting as carbon sink, confirmed previous studies that the mid- and high latitudes in the Northern Hemisphere have strong carbon sequestration capacity (Tans *et al*., 1990; Ciais *et al*., 2000; Hayes *et al*., 2011). The average value of NEP was higher than that in the United States and Europe in magnitude (Fig. 3c). However, this difference was not statistically significant ($P > 0.05$). This result was different from the study of Piao *et al*. (2009), who found the sink magnitude in China was similar to that in Europe but lower than that in the United States.

The average value of NEP of forest ecosystems in China was higher than those in Europe, the United States, and Canada. However, this difference among China, Europe, and the United States was not significant at the significant level of 0.05, which was also found in GEP, while there was no significant difference in ER for the forest ecosystems among the above four regions. This indicates that the difference in NEP of forest ecosystems in these four regions mainly resulted from the difference of GEP. This was possibly resulted from the low MAT in Canada at high latitudes, which limited GEP and in turn NEP.

There was no statistical significant difference in NEP of grassland ecosystems among different regions, whereas the GEP values of grasslands in Europe and the United States were significantly higher than those in China and Canada. This difference was mainly associated with the grassland types and their management practices. In Europe, grasslands are distributed in the areas with favorable hydrothermal conditions, most of which were under intensive management, leading to a higher productivity (Gilmanov *et al*., 2007; Jacobs *et al*., 2007; Soussana *et al*., 2007). However, the GEP and NEP of grasslands in China were generally lower than these in the United States and Europe. This was partly because the grasslands in this study are mostly located in arid or alpine areas in northern China (Fan *et al*., 2008), which are subject to the constraint of rainfall or temperature and high pressure of grazing (Fu *et al*., 2009).

The carbon fluxes of wetlands and croplands showed no significant difference among regions. This is because the wetlands are scatteredly distributed worldwide with influences of complex human activities (Whigham, 2009), while the croplands are highly subjected to the intensity of human managements and cropping systems (Ramankutty *et al*., 2002).

It should be noted that all the above results were only the summary on the data measured at the existing sites. Meanwhile, some climate zones only had one or two observations, which limited the evaluation of the uncertainty but could not overcome currently. Considering the number and spatial representation of observation sites in different regions, our findings need to be further validated with more observation results.

Phenomenon of the 'positive coupling correlation' in GEP, ER, and NEP

The correlation among the seasonal dynamics of GEP, ER, and NEP in some regions has been extensively

demonstrated (Lasslop *et al.*, 2010). It is generally believed that the environmental drivers of GEP and ER have similar dynamic processes in the seasonal or interannual changes. Meanwhile, GEP, as the main substrate supplier of ER, will inevitably constrain the variation of ER. Therefore, GEP and ER exhibited a highly 'positive coupling correlation' in the process of seasonal or interannual variation (Law *et al.*, 2002; Stoy *et al.*, 2007). However, the positive correlation between NEP (the small difference between GEP and ER) and GEP would appear when ER remaining relatively stable. In general, GEP is larger than ER during the growing seasons in boreal forest and grassland ecosystems, and the growth rate of GEP is much larger than that of ER (e.g., Guan *et al.*, 2006; Humphreys *et al.*, 2006; Jaksic *et al.*, 2006). This results in the positive correlation between NEP and GEP, i.e., the peak season of GEP is also that of NEP (e.g., Flanagan *et al.*, 2002; Jaksic *et al.*, 2006).

There are very few studies about the correlation of spatial patterns of GEP, ER, and NEP (Law *et al.*, 2002; Van Dijk & Dolman, 2004; Baldocchi, 2008). In this study, we found a surprising phenomenon that not only ER but also NEP showed obvious 'positive coupling correlation' (Fig. 5) with GEP in their spatial patterns across all terrestrial ecosystems in China (consisting of forest, grassland, wetland, and cropland ecosystems), which can be well described with Eqns (4) and (5) as follows:

$$\mathrm{ER} = 0.68\mathrm{GEP} + 81.90, R^2 = 0.90, n = 41 \quad (4)$$

$$\mathrm{NEP} = 0.29\mathrm{GEP} - 37.22, R^2 = 0.57, n = 39 \quad (5)$$

The previous study has suggested that the ER of forest ecosystems in Europe grew in an exponential way with the increase of GEP (Van Dijk & Dolman, 2004), while at global scale 77% of GEP was respired through ER (Baldocchi, 2008). Law *et al.* (2002) found that NEP grew linearly with the increase of GEP in forest ecosystems in Europe and the United States, with 44%–67% of GEP contributed to NEP. In this study, we found that both ER and NEP grew with GEP linearly, with 68% of GEP contributed to ER and 29% to NEP. The relatively low contribution of GEP to NEP in China was possibly because our study combined several vegetation types together, while their studies only focused on forest ecosystems that usually had higher carbon use efficiency (NEP/GPP) than other ecosystem types.

The underlying mechanism of the tight correlation among GEP, ER, and NEP in spatial patterns might be similar with the close correlation relationship among GEP, ER, and NEP in temporal (seasonal and interannual) dynamics. This could be attributed to the following aspects. On one hand, the spatial patterns of GEP, ER, and NEP were codetermined by MAT and MAP, and their responding trends to the variation of MAT and MAP were similar. On the other hand, at annual scale, ER was primarily constrained by GEP, which was the main substrate supplier of ER.

Climatic factors control on the spatial patterns of GEP, ER, and NEP

The regional climate in China is characterized by complex zonal changes, not only in horizontal direction (latitudinal and longitudinal) but also in vertical direction (altitudinal). This leads to the complex spatial patterns of GEP, ER, and NEP (Fig. 4). Our results indicate that the spatial patterns of GEP, ER, and NEP of terrestrial ecosystem in China were largely determined by MAT and MAP not only independently but also interactively. This is mainly associated with the latitudinal patterns of MAT and MAP in China (Fig. 2).

GEP, ER, and NEP in different ecosystems (i.e., forest, grassland, and wetland) are significantly correlated with MAT and MAP. This is consistent with the conclusions of previous studies in the same (Yu *et al.*, 2008; Fu *et al.*, 2009) or other regions (Law *et al.*, 2002; Luyssaert *et al.*, 2007; Wang *et al.*, 2008). A surprising finding was that GEP, ER, and NEP varied consistently with the changes in MAT and MAP (Fig. 7), which can be described with a similar function (Formulas 1-3). This suggests that although the carbon fluxes from various ecosystems may respond to the changes in MAT and MAP differently, these variances were not strong enough to alter the basic law that spatial patterns of GEP, ER, and NEP were determined by MAT and MAP.

Based on the above analyses, we can infer the underlying mechanism of the spatial patterns of carbon fluxes in terrestrial ecosystems in China. Firstly, the complex regional topography and monsoon climate in China have shaped the spatial variations of MAT and MAP, which, in turn, jointly determined the distinct latitudinal patterns and complex longitudinal patterns of GEP, ER, and NEP. Secondly, the spatial patterns of ER and NEP showed a high 'positive coupling correlation' with that of GEP. Thirdly, MAT and MAP controlled the spatial patterns of carbon fluxes mainly by their direct effects on GEP and subsequent indirect effects on ER and NEP. This was different from the result that ER dominated the spatial pattern of NEP in European forest ecosystems (Valentini *et al.*, 2000).

Acknowledgements

This research was supported by the National Key Research and Development Program (2010CB833504), the CAS Strategic Priority Research Program (grant no. XDA05050602), and National

Natural Science Foundation of China (31290220, 30900198). We gratefully acknowledge the reviewers for spending their valuable time to provide constructive comments.

References

Anderson-Teixeira KJ, Delong JP, Fox AM, Brese DA, Litvak ME (2011) Differential responses of production and respiration to temperature and moisture drive the carbon balance across a climatic gradient in New Mexico. *Global Change Biology*, **17**, 410–424.

Baldocchi D (2008) Breathing of the terrestrial biosphere: Lessons learned from a global network of carbon dioxide flux measurement systems. *Australian Journal of Botany*, **56**, 1–26.

Baldocchi D, Falge E, Gu LH *et al.* (2001) FLUXNET: A new tool to study the temporal and spatial variability of ecosystem-scale carbon dioxide, water vapor, and energy flux densities. *Bulletin of the American Meteorological Society*, **82**, 2415–2434.

Beer C, Reichstein M, Tomelleri E *et al.* (2010) Terrestrial gross carbon dioxide uptake: Global distribution and covariation with climate. *Science*, **329**, 834–838.

Bracho R, Starr G, Gholz HL, Martin TA, Cropper WP, Loescher HW (2012) Controls on carbon dynamics by ecosystem structure and climate for southeastern U.S. slash pine plantations. *Ecological Monographs*, **82**, 101–128.

Canadell JG, Mooney HA, Baldocchi DD *et al.* (2000) Carbon metabolism of the terrestrial biosphere: A multitechnique approach for improved understanding. *Ecosystems*, **3**, 115–130.

Cao M, Yu G, Liu J, Li K (2005) Multi-scale observation and cross-scale mechanistic modeling on terrestrial ecosystem carbon cycle. *Science in China Series D-Earth Sciences*, **48**, 17–32.

Chapin FS, Woodwell GM, Randerson JT *et al.* (2006) Reconciling carbon-cycle concepts, terminology, and methods. *Ecosystems*, **9**, 1041–1050.

Chapin FS, Mcfarland J, Mcguire AD, Euskirchen ES, Ruess RW, Kielland K (2009) The changing global carbon cycle: linking plant-soil carbon dynamics to global consequences. *Journal of Ecology*, **97**, 840–850.

Chen BZ, Chen JM, Mo G, Black A, Worthy DEJ (2008) Comparison of regional carbon flux estimates from CO_2 concentration measurements and remote sensing based footprint integration. *Global Biogeochemical Cycles*, **22**, GB2012, doi: 10.1029/2007gb003024.

Ciais P, Peylin P, Bousquet P (2000) Regional biospheric carbon fluxes as inferred from atmospheric CO_2 measurements. *Ecological Applications*, **10**, 1574–1589.

Deng F, Chen JM (2011) Recent global CO_2 flux inferred from atmospheric CO_2 observations and its regional analyses. *Biogeosciences*, **8**, 3263–3281.

Ding YH, Chan JCL (2005) The East Asian summer monsoon: an overview. *Meteorology and Atmospheric Physics*, **89**, 117–142.

Falge E, Baldocchi D, Olson R *et al.* (2001) Gap filling strategies for defensible annual sums of net ecosystem exchange. *Agricultural and Forest Meteorology*, **107**, 43–69.

Falkowski P, Scholes RJ, Boyle E *et al.* (2000) The global carbon cycle: a test of our knowledge of earth as a system. *Science*, **290**, 291–296.

Fan J, Zhong H, Harris W, Yu G, Wang S, Hu Z, Yue Y (2008) Carbon storage in the grasslands of China based on field measurements of above- and below-ground biomass. *Climatic Change*, **86**, 375–396.

Fang JY, Guo ZD, Piao SL, Chen AP (2007) Terrestrial vegetation carbon sinks in China, 1981-2000. *Science in China Series D-Earth Sciences*, **50**, 1341–1350.

Flanagan LB, Wever LA, Carlson PJ (2002) Seasonal and interannual variation in carbon dioxide exchange and carbon balance in a northern temperate grassland. *Global Change Biology*, **8**, 599–615.

Fu Y, Yu G, Wang Y, Li Z, Hao Y (2006) Effect of water stress on ecosystem photosynthesis and respiration of a *Leymus chinensis* steppe in Inner Mongolia. *Science in China Series D-Earth Sciences*, **49**, 196–206.

Fu Y, Zheng Z, Yu G *et al.* (2009) Environmental influences on carbon dioxide fluxes over three grassland ecosystems in China. *Biogeosciences*, **6**, 2879–2893.

Gilmanov TG, Soussana JE, Aires L *et al.* (2007) Partitioning European grassland net ecosystem CO_2 exchange into gross primary productivity and ecosystem respiration using light response function analysis. *Agriculture Ecosystems & Environment*, **121**, 93–120.

Guan DX, Wu JB, Zhao XS, Han SJ, Yu GR, Sun XM, Jin CJ (2006) CO_2 fluxes over an old, temperate mixed forest in northeastern China. *Agricultural and Forest Meteorology*, **137**, 138–149.

Hao Y, Wang Y, Sun X *et al.* (2006) Seasonal variation in carbon exchange and its ecological analysis over *Leymus chinensis* steppe in Inner Mongolia. *Science in China Series D-Earth Sciences*, **49**, 186–195.

Hayes DJ, Mcguire AD, Kicklighter DW, Gurney KR, Burnside TJ, Melillo JM (2011) Is the northern high-latitude land-based CO_2 sink weakening? *Global Biogeochemical Cycles*, **25**, GB3018, doi: 10.1029/2010gb003813.

Hirata R, Saigusa N, Yamamoto S *et al.* (2008) Spatial distribution of carbon balance in forest ecosystems across East Asia. *Agricultural and Forest Meteorology*, **148**, 761–775.

Houghton RA (2007) Balancing the global carbon budget. *Annual Review of Earth and Planetary Sciences*, **35**, 313–347.

Humphreys ER, Black TA, Morgenstern K, Cai TB, Drewitt GB, Nesic Z, Trofymow JA (2006) Carbon dioxide fluxes in coastal *Douglas-fir* stands at different stages of development after clearcut harvesting. *Agricultural and Forest Meteorology*, **140**, 6–22.

Jacobs CMJ, Jacobs AFG, Bosveld FC *et al.* (2007) Variability of annual CO_2 exchange from Dutch grasslands. *Biogeosciences*, **4**, 803–816.

Jaksic V, Kiely G, Albertson J, Oren R, Katul G, Leahy P, Byrne KA (2006) Net ecosystem exchange of grassland in contrasting wet and dry years. *Agricultural and Forest Meteorology*, **139**, 323–334.

Jung M, Reichstein M, Margolis HA *et al.* (2011) Global patterns of land-atmosphere fluxes of carbon dioxide, latent heat, and sensible heat derived from eddy covariance, satellite, and meteorological observations. *Journal of Geophysical Research*, **116**, G00J07 doi: 10.1029/2010jg001566.

Kato T, Tang YH (2008) Spatial variability and major controlling factors of CO_2 sink strength in Asian terrestrial ecosystems: evidence from eddy covariance data. *Global Change Biology*, **14**, 2333–2348.

Keller M, Alencar A, Asner GP *et al.* (2004) Ecological research in the large-scale biosphere- atmosphere experiment in Amazonia early results. *Ecological Applications*, **14**, 3–16.

Lasslop G, Reichstein M, Papale D *et al.* (2010) Separation of net ecosystem exchange into assimilation and respiration using a light response curve approach: critical issues and global evaluation. *Global Change Biology*, **16**, 187–208.

Law BE, Falge E, Gu L *et al.* (2002) Environmental controls over carbon dioxide and water vapor exchange of terrestrial vegetation. *Agricultural and Forest Meteorology*, **113**, 97–120.

Leuning R, Yu GR (2006) Carbon exchange research in ChinaFLUX. *Agricultural and Forest Meteorology*, **137**, 123–124.

Li Z, Yu G, Wen X, Zhang L, Ren C, Fu Y (2005) Energy balance closure at ChinaFLUX sites. *Science in China Series D-Earth Sciences*, **48**, 51–62.

Li Y, Sun X, Zhao X *et al.* (2006) Seasonal variations and mechanism for environmental control of NEE of CO_2 concerning the *Potentilla fruticosa* in alpine shrub meadow of Qinghai-Tibet Plateau. *Science in China Series D-Earth Sciences*, **49**, 174–185.

Liu YH, Ge QS, He FN, Cheng BB (2008) Countermeasures against international pressure of reducing CO_2 emissions and analysis on China's potential of CO_2 emission reduction. *Acta Geographica Sinica*, **63**, 675–682 (in Chinese with English abstract).

Lund M, Lafleur PM, Roulet NT *et al.* (2010) Variability in exchange of CO_2 across 12 northern peatland and tundra sites. *Global Change Biology*, **16**, 2436–2448.

Luyssaert S, Inglima I, Jung M *et al.* (2007) CO_2 balance of boreal, temperate, and tropical forests derived from a global database. *Global Change Biology*, **13**, 2509–2537.

Massman WJ, Lee X (2002) Eddy covariance flux corrections and uncertainties in long-term studies of carbon and energy exchanges. *Agricultural and Forest Meteorology*, **113**, 121–144.

Pan Y, Birdsey RA, Fang J *et al.* (2011) A large and persistent carbon sink in the world's forests. *Science*, **333**, 988–993.

Piao S, Fang J, Ciais P, Peylin P, Huang Y, Sitch S, Wang T (2009) The carbon balance of terrestrial ecosystems in China. *Nature*, **458**, 1009–1013.

Ramankutty N, Foley JA, Norman J, Mcsweeney K (2002) The global distribution of cultivable lands: current patterns and sensitivity to possible climate change. *Global Ecology and Biogeography*, **11**, 377–392.

Reichstein M, Falge E, Baldocchi D *et al.* (2005) On the separation of net ecosystem exchange into assimilation and ecosystem respiration: review and improved algorithm. *Global Change Biology*, **11**, 1424–1439.

Royden LH, Burchfiel BC, Van Der Hilst RD (2008) The geological evolution of the tibetan plateau. *Science*, **321**, 1054–1058.

Solomon S, Qin D, Manning M *et al.* (2007) *Climate Change 2007: The Physical Science Basis, Contribution of Working Group 1 to the Fourth Assessment Report of the Intergovernmental Panel on Climate Change*, United Kingdom Cambridge University Press, Cambridge.

Soussana JF, Allard V, Pilegaard K *et al.* (2007) Full accounting of the greenhouse gas (CO_2, N_2O, CH_4) budget of nine European grassland sites. *Agriculture Ecosystems & Environment*, **121**, 121–134.

Stoy PC, Palmroth S, Oishi AC *et al.* (2007) Are ecosystem carbon inputs and outputs coupled at short time scales? A case study from adjacent pine and hardwood forests using impulse-response analysis. *Plant Cell and Environment*, **30**, 700–710.

Tan Z, Zhang Y, Yu G, Sha L, Tang J, Deng X, Song Q (2010) Carbon balance of a primary tropical seasonal rain forest. *Journal of Geophysical Research*, **115**, D00H26, doi: 10.1029/2009jd012913.

Tan ZH, Zhang YP, Schaefer D, Yu GR, Liang N, Song QH (2011) An old-growth subtropical Asian evergreen forest as a large carbon sink. *Atmospheric Environment*, **45**, 1548–1554.

Tans PP, Fung IY, Takahashi T (1990) Observational contrains on the global atmospheric CO_2 budget. *Science*, **247**, 1431–1438.

Valentini R, Matteucci G, Dolman AJ *et al.* (2000) Respiration as the main determinant of carbon balance in European forests. *Nature*, **404**, 861–865.

Van Dijk A, Dolman AJ (2004) Estimates of CO_2 uptake and release among European forests based on eddy covariance data. *Global Change Biology*, **10**, 1445–1459.

Wang XC, Wang CK, Yu GR (2008) Spatio-temporal patterns of forest carbon dioxide exchange based on global eddy covariance measurements. *Science in China Series D-Earth Sciences*, **51**, 1129–1143.

Webb EK, Pearman GL, Leuning R (1980) Correction of flux measurement for density effects due to heat and water vapor transfer. *Quarterly Journal of Royal Meteorological Society*, **106**, 85–100.

Wen XF, Yu GR, Sun XM, Liu YF (2005) Turbulence flux measurement above the overstory of a subtropical Pinus plantation over the hilly region in southeastern China. *Science in China Series D-Earth Sciences*, **48**, 63–73.

Wen XF, Wang HM, Wang JL, Yu GR, Sun XM (2010) Ecosystem carbon exchanges of a subtropical evergreen coniferous plantation subjected to seasonal drought, 2003-2007. *Biogeosciences*, **7**, 357–369.

Whigham DF (2009) Global distribution, diversity and human alterations of wetland resources. In: *The Wetlands Handbook* (eds Maltby E, Baker T), pp. 43–64. Wiley-Blackwell, Singapore.

Wilson K, Goldstein A, Falge E *et al.* (2002) Energy balance closure at FLUXNET sites. *Agricultural and Forest Meteorology*, **113**, 223–243.

Wu GX, Liu YM, Wang TM *et al.* (2007) The influence of mechanical and thermal forcing by the Tibetan Plateau on Asian climate. *Journal of Hydrometeorology*, **8**, 770–789.

Xiao JF, Zhuang QL, Baldocchi DD *et al.* (2008) Estimation of net ecosystem carbon exchange for the conterminous United States by combining MODIS and AmeriFlux data. *Agricultural and Forest Meteorology*, **148**, 1827–1847.

Xiao JF, Zhuang QL, Law BE *et al.* (2010) A continuous measure of gross primary production for the conterminous United States derived from MODIS and AmeriFlux data. *Remote Sensing of Environment*, **114**, 576–591.

Xiao J, Zhuang Q, Law BE *et al.* (2011) Assessing net ecosystem carbon exchange of U.S. terrestrial ecosystems by integrating eddy covariance flux measurements and satellite observations. *Agricultural and Forest Meteorology*, **151**, 60–69.

Yi CX, Ricciuto D, Li R *et al.* (2010) Climate control of terrestrial carbon exchange across biomes and continents. *Environmental Research Letters*, **5**, 034007, doi: 10.1088/1748-9326/5/3/034007.

Yu GR, Wen XF, Sun XM, Tanner BD, Lee X, Chen JY (2006a) Overview of ChinaFLUX and evaluation of its eddy covariance measurement. *Agricultural and Forest Meteorology*, **137**, 125–137.

Yu GR, Fu YL, Sun XM, Wen XF, Zhang LM (2006b) Recent progress and future directions of ChinaFLUX. *Science in China Series D-Earth Sciences*, **49**, 1–23.

Yu GR, Zhang LM, Sun XM *et al.* (2008) Environmental controls over carbon exchange of three forest ecosystems in eastern China. *Global Change Biology*, **14**, 2555–2571.

Yu G, Zheng Z, Wang Q, Fu Y, Zhuang J, Sun X, Wang Y (2010) Spatiotemporal pattern of soil respiration of terrestrial ecosystems in China: the development of a geostatistical model and its simulation. *Environmental Science & Technology*, **44**, 6074–6080.

Yu GR, Fang HJ, Fu YL, Wang QF (2011a) Research on carbon budget and carbon cycle of terrestrial ecosystems in regional scale: a review. *Acta Ecologica Sinica*, **31**, 5449–5459 (in Chinese with English abstract).

Yu GR, Wang QF, Zhu XJ (2011b) Methods and uncertainties in evaluating the carbon budgets of regional terrestrial ecosystems. *Progress in Geography*, **30**, 103–113 (in Chinese with English abstract).

Yuan WP, Liu SG, Yu GR *et al.* (2010) Global estimates of evapotranspiration and gross primary production based on MODIS and global meteorology data. *Remote Sensing of Environment*, **114**, 1416–1431.

Zhang J, Yu G, Han S, Guan D, Sun X (2006) Seasonal and annual variation of CO_2 flux above a broad-leaved Korean pine mixed forest. *Science in China Series D-Earth Sciences*, **49**, 63–73.

Zhu ZL, Sun XM, Zhou YL, Xu JP, Yuan GF, Zhang RH (2005) Correcting method of eddy covariance fluxes over non-flat surfaces and its application in ChinaFLUX. *Science in China Series D-Earth Sciences*, **48**, 42–50.

Zhu X, He H, Liu M, Yu G, Sun X, Gao Y (2010) Spatio-temporal variation of photosynthetically active radiation in China in recent 50 years. *Journal of Geographical Sciences*, **20**, 803–817.

Supporting Information

Additional Supporting Information may be found in the online version of this article:

Table S1. Sites information used in this study.